Journal of
Composites Science

MDPI

Article

The Effect of Lubricant and Nanofiller Additives on Drilling Temperature in GFRP Composites

Mohamed Slamani [1,2], Jean-François Chatelain [2,*] and Siwar Jammel [2]

[1] Mechanical Engineering Department, Faculty of Technology, University of M'sila, University Pole, Road Bourdj Bou Arreiridj, M'sila 28000, Algeria; mohamed.slamani@univ-msila.dz
[2] Mechanical Engineering Department, École de Technologie Supérieure, 1100 Notre-Dame West St, Montreal, QC H3C 1K3, Canada; siwarjammel5@gmail.com
* Correspondence: jean-francois.chatelain@etsmtl.ca

Abstract

Glass fiber-reinforced polymer (GFRP) composites are highly susceptible to thermal damage during machining, which can compromise their structural integrity and final quality. This study examines the efficacy of graphene and wax additives in reducing drilling temperatures in GFRP composites. Nine unique samples were manufactured with varying weight percentages of wax (0%, 1%, 2%) and graphene (0%, 0.25%, 2%). Drilling experiments were performed on a CNC milling center under a range of cutting parameters, with temperature monitoring carried out using an infrared thermal camera. A hierarchical cubic response surface model was employed to analyze thermal behavior. The results indicate that cutting speed is the dominant factor, accounting for 67.28% of temperature generation. The formulation containing 2% wax and 0% graphene achieved the lowest average drilling temperature (64.64 °C), underscoring wax's superior performance as both a lubricant and heat sink. Although graphene alone slightly elevated median temperatures, it substantially reduced thermal variability. The optimal condition for minimizing thermal damage was identified as 2% wax combined with a high cutting speed (200 mm/min), providing actionable insights for industrial process optimization.

Keywords: glass fiber-reinforced polymer (GFRP); machining; drilling temperature; graphene; wax; additive manufacturing; response surface methodology; process optimization; thermal analysis

Academic Editors: Xiangfa Wu and Oksana Zholobko

Received: 19 September 2025
Revised: 6 October 2025
Accepted: 10 October 2025
Published: 12 October 2025

Citation: Slamani, M.; Chatelain, J.-F.; Jammel, S. The Effect of Lubricant and Nanofiller Additives on Drilling Temperature in GFRP Composites. *J. Compos. Sci.* **2025**, *9*, 558. https://doi.org/10.3390/jcs9100558

1. Introduction

Drilling glass fiber-reinforced polymer (GFRP) composites is essential in aerospace, automotive, and wind energy industries, where maintaining precision and structural integrity is critical [1]. However, their heterogeneous and anisotropic structure makes them susceptible to drilling-induced defects such as delamination, fiber pull-out, and matrix degradation [2]. Due to the low thermal conductivity of epoxy (~0.3–0.6 W/m·°C), heat accumulation can easily exceed the glass transition temperature (Tg), compromising hole quality [1]. Optimizing spindle speed and feed rate is therefore vital for minimizing thermal and mechanical damage [3,4]. Reyhan et al. [2] reported that feed rate and cooling strategy strongly influence drilling quality, with cryogenic cooling improving performance. Malik et al. [1] found that low feed and high speed reduce drilling defects, while Mudegowdar [5] confirmed the sensitivity of thermal and mechanical responses to these parameters. Similarly, Jessy et al. [6] showed that using internal coolant lowered drill temperature by

up to 76% compared to dry drilling, enhancing tool life by 43.75% and enabling accurate temperature prediction (±7% error).

Several studies have systematically analyzed drilling parameters to mitigate damage in composites. Biruk-Urban et al. [7] identified feed per tooth as the most critical factor for delamination in thin GFRP, while Tian et al. [8] detailed how tool geometry and cutting parameters interact to cause exit damage. For nanocomposites, Thangavel et al. [9] demonstrated that nanoparticle concentration is the dominant parameter, significantly influencing thrust force and surface roughness. Comprehensive reviews by Zhu et al. [10] and on temperature dynamics and others on hybrid stacks [11] further underscore the complex thermal-mechanical challenges in drilling composite materials.

Machine learning is increasingly used to predict machining outcomes for composites. For instance, artificial neural networks have accurately predicted milling temperatures in GFRPs from cutting parameters [12], while other models have related feed rate and speed to drilling forces and delamination [13].

In parallel, sustainable cooling methods have advanced significantly. Pereira et al. [14–16] developed and optimized hybrid systems combining cryogenic CO_2 cooling with minimum quantity lubrication (MQL), demonstrating notable improvements in heat dissipation, tool life, and surface quality. Their CryoMQL systems, featuring optimized nozzle designs and integrated CO_2–MQL flow, achieved a successful balance between technical performance and environmental responsibility during the machining of difficult-to-cut alloys such as Inconel 718. Complementing these external methods, material-based strategies incorporate solid lubricants or thermally conductive fillers like graphene, CNTs, or boron nitride into the composite matrix [17]. These additives have been shown to enhance thermal conductivity [18,19], improve wear resistance [17] and enable tunable thermal properties [20].

However, the effectiveness of such strategies is not universal. Unal et al. [21] reported that certain filler concentrations can increase thrust force and temperature due to particle agglomeration. Xu et al. [22] emphasized the need for improved cooling to counter intense localized frictional heat, while Zitoune et al. [23] demonstrated the significant role of tool coatings in controlling temperature and wear. Maintaining structural integrity post-drilling is critical, as shown by studies on flexural and interlaminar strength [24]. The influence of machining parameters on overall composite behavior [25], delamination mechanisms [26], and high-speed drilling effects [27] further underscores the complex thermo-mechanical challenges involved.

Sorrentino et al. [28] utilized real-time thermal monitoring to reveal dynamic temperature evolution adversely affecting hole quality. Chen's early research [29] examined damage propagation across different tool geometries, while Rawat & Attia [30] investigated wear and tool-life challenges in dry high-speed drilling of carbon composites, highlighting thermal loading's critical role. Meshreki et al. [31] assessed cooling methods for multilayer stacks, establishing cooling as essential for thermal damage mitigation. Giasin et al. [32] demonstrated cryogenic LN_2's superiority over MQL through significant reductions in thrust force and surface roughness.

Renteria et al. [33] pioneered graphene as a self-aligning thermal filler for passive temperature control. Subsequent reviews by Khan & Balandin [34] and Gulotty et al. [35] reinforced the advantages of graphene and CNT dispersions for thermal management.

Xian et al. [36] developed a self-healing epoxy composite using carbon nanotubes (CNTs) and polycaprolactone (PCL). The optimal formula with 0.5% CNTs and 5% PCL increased tensile strength by 25.4% and elongation by 42.3%. The material demonstrated excellent self-repair, with healing efficiency reaching 116.1% after three cycles, as PCL melted to bridge and heal micro-cracks. Barani et al. [37] achieved enhanced thermal conductivity

in graphene–copper hybrid composites, while El-Ghaoui et al. [38] specifically documented graphene's benefits in GFRP machining, observing reduced cutting temperatures and superior surface finishes. Palanikumar et al. [39] employed grey relational analysis to establish correlations between machining parameters and drilling outcomes.

While graphene additives are known to enhance thermal conductivity in polymers [40,41] and solid lubricants like wax reduce frictional heating in machining [17], their combined effects in composite drilling remain unexplored. This study addresses this gap by systematically investigating simultaneous graphene and wax incorporation in GFRP composites. Through controlled drilling experiments and predictive modeling, a novel framework is established for identifying optimal additive combinations that minimize thermal damage in fiber-reinforced composites.

Building upon this foundation of thermal management research, the primary objective of this work is to systematically investigate the individual and combined effects of wax and graphene additives, feed rate, and cutting speed on both the central tendency (median) and variability (IQR) of drilling temperatures in GFRP composites. Using a full factorial design, this study aims to address the critical gap in understanding how these parameters influence not only average thermal behavior but also process reproducibility, thereby providing actionable insights for minimizing thermal damage and enhancing drilling precision in composite manufacturing.

2. Materials and Methods

2.1. Materials

2.1.1. Sample Preparation

This study involved the fabrication of glass fiber-reinforced polymer (GFRP) specimens incorporating varying proportions of graphene and wax to assess their influence on machining behavior. Graphene (Graphene Black 0X) and wax (Ceraflour 996) were sourced from Nano-Xplore Inc (Montreal, Quebec, Canada) and BYK USA Inc (Wallingford, CT, USA), respectively. These additives were blended into a Marine 820 epoxy resin matrix, which served as the binding medium for the composite system.

The use of nanofiller additives, particularly graphene, raises concerns regarding potential occupational health risks. Previous studies have shown that inhalation of airborne nanoparticles may pose respiratory hazards and lead to adverse health outcomes if exposure is not properly controlled [42,43]. Although wax additives are generally considered safe, handling graphene powders requires strict safety measures, including the use of fume hoods, personal protective equipment (PPE), and proper waste disposal procedures. In industrial practice, these risks can be effectively mitigated by implementing engineering controls and following established nanosafety guidelines [44]. Thus, while the functional benefits of graphene are clear, attention to safe processing and handling is essential to ensure worker protection during material preparation and machining operations.

Nine distinct GFRP samples were prepared by varying the weight percentages of wax and graphene. The formulations included three levels of wax (0%, 1%, and 2%) and three levels of graphene (0%, 0.25%, and 2%). The combinations were as follows (Figure 1):

- Samples 1–3 contained no wax, with graphene levels of 0%, 0.25%, and 2%, respectively.
- Samples 4–6 incorporated 1% wax, paired with the same increasing concentrations of graphene (0%, 0.25%, and 2%).
- Samples 7–9 featured 2% wax, again matched with 0%, 0.25%, and 2% graphene.

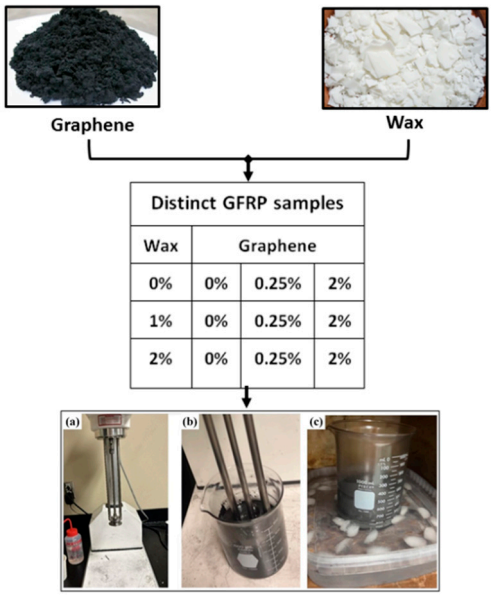

Figure 1. Sample preparation.

The selection of graphene concentrations (0%, 0.25%, and 2%) was informed by prior findings indicating that even very low graphene loadings (around 0.1%) can yield significant improvements in tensile strength and modulus while avoiding issues such as agglomeration and matrix degradation [45]. However, as reported by Cui et al. [46], further increasing the graphene content beyond approximately 2 wt % can lead to diminishing or even adverse effects on mechanical performance due to filler agglomeration and interfacial defects. Accordingly, 0.25% was selected to represent a low-to-intermediate regime where property enhancement begins, and 2% as an upper limit that remains below the threshold at which excessive clustering typically occurs. Although including additional intermediate loadings could provide finer resolution, the three chosen levels offer a practical yet representative range to capture the transition from low to higher graphene content regimes.

To achieve uniform dispersion of the additives, the mixture was processed using a Silverson L5M-A high-shear mixer (Silverson Machines, Inc., East Longmeadow, MA, USA). The mixing protocol consisted of six sequential steps, four at 2 min each and two at 3 min with rotational speeds increasing from 1500 to 10,000 revolutions per minute (RPM). This gradual escalation in shear force was designed to maximize dispersion quality and reduce agglomeration.

To maintain the mixture's thermal integrity and prevent exceeding the epoxy's glass transition temperature, the vessel was cooled using an ice bath, keeping the temperature below 30 °C throughout mixing (Figure 1). This control was especially important during the final two stages, where increased speeds could generate more heat. The resulting lower viscosity also facilitated more effective air removal during degassing.

Degassing was performed in two stages. The first occurred immediately after mixing, under vacuum conditions for one hour at a pressure of 29 inHg, which was necessary to extract the air trapped during the intense mixing phase. The second stage followed the introduction of the curing agent and involved a gentler vacuum treatment for 15 min to avoid reintroducing bubbles.

2.1.2. Laminate Fabrication

Hand lay-up molding was selected for its simplicity and economic feasibility. The mold base was lined with a non-stick film and coated with a release agent to facilitate easy demolding. Glass fiber layers were stacked manually, with each layer impregnated

with the prepared epoxy mixture and pressed using a roller to eliminate trapped air and prevent delamination. Up to 16 layers were applied, with fibers oriented at alternating angles (±90°) to enhance structural uniformity (Figure 2a).

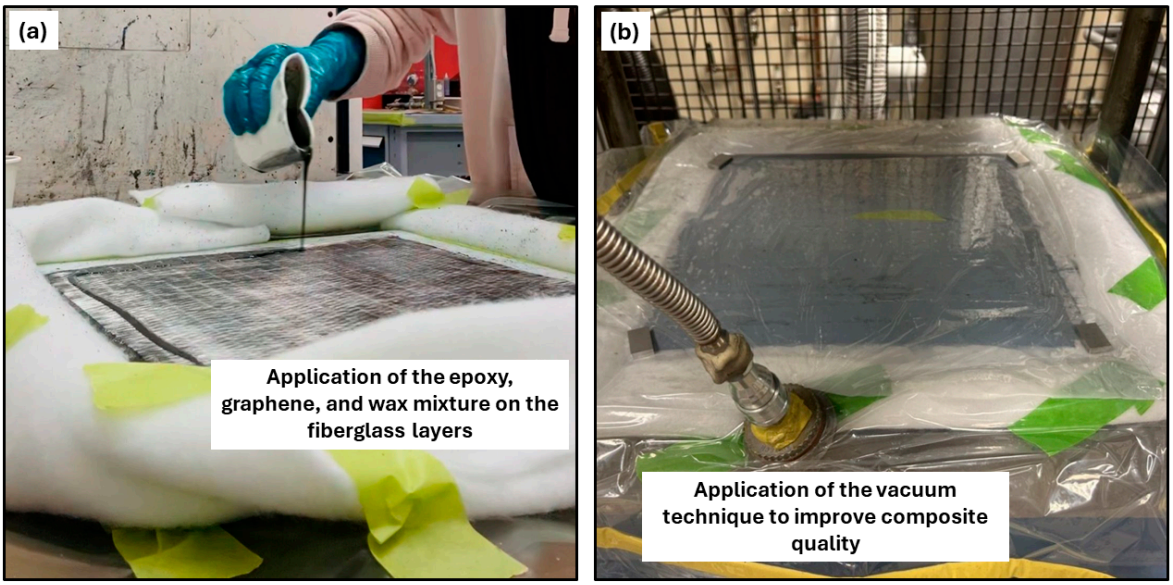

Figure 2. Preparation of the composite laminates.

Once lay-up was complete, the laminate was enclosed in a vacuum bag to improve fiber–resin consolidation (Figure 2b). It was then compressed at 60 °C using a hydraulic press, with 5 mm spacers installed to maintain consistent thickness across samples. Each panel was 12 inches by 12 inches in dimension and was used for subsequent machining experiments.

2.1.3. Drilling Procedure

Machining trials were performed using a Huron K2X10 three-axis CNC milling center, capable of reaching 28,000 RPM and offering a power output of 40 kW (Figure 3a). The drilling operations were conducted using a chemical vapor deposition (CVD)-coated twist drill (COREHOG) with a diameter of 5.5 mm, selected for its durability under high-speed cutting conditions (Figure 3b).

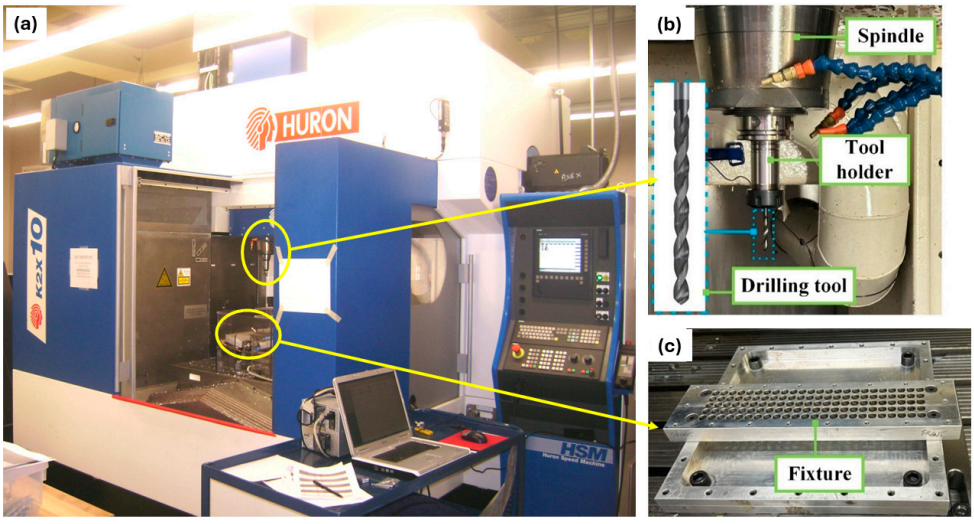

Figure 3. (**a**) Huron K2X10 three-axis CNC milling center, (**b**) drilling setup using CVD-coated drill, (**c**) drilling fixture.

The tool was characterized by its main geometric parameters, consistent with standard twist drill geometry used in composite machining: point angle of 118°, helix angle of 30°, lip relief angle of 12°, and web thickness of 0.25 mm. These geometrical features are critical as they influence chip evacuation, cutting forces, and thermal generation during the drilling of composite laminates.

The drilling experiments were conducted under four distinct machining settings, each defined by a specific pairing of cutting speed and feed rate. The selected cutting velocities were 50, 100, 150, and 200 mm/min (corresponding to 0.05, 0.10, 0.15, and 0.20 m/min). The feed rates were set at 0.02, 0.04, 0.06, and 0.08 mm/rev, respectively. This structured variation allowed for the systematic evaluation of machining performance across a broad range of cutting intensities.

To ensure stability and precision during drilling, a dedicated machining fixture was specifically designed and fabricated for this test, as shown in Figure 3c. Each GFRP plate was drilled following a predefined path, with three repeated holes (T1, T2, T3) produced for each cutting condition to ensure consistency and facilitate statistical analysis. The same drilling sequence was applied uniformly across all nine sample types.

During the drilling operations, surface temperature measurements were acquired using a VarioCAM® HD head 900 infrared thermal camera, capable of high-resolution, non-contact thermal imaging. This system enabled real-time monitoring of the temperature distribution on the GFRP sample surface. The collected thermal data were subsequently processed and analyzed to examine the influence of varying graphene and wax content on the thermal behavior of the material under different cutting conditions. Monitoring the temperature profile during drilling is essential for assessing heat generation, which can affect tool wear, matrix degradation, and machining performance. It is important to note that emissivity plays a decisive role in determining the accuracy of infrared-based surface temperature measurements. Variations in emissivity within the heterogeneous glass–epoxy matrix, along with subsurface heat distribution, may introduce some deviation from true absolute values. Therefore, the recorded temperatures in this study are most reliable for relative comparisons between additives and cutting conditions rather than as precise absolute measurements. The experimental setup used for temperature monitoring is illustrated in Figure 4.

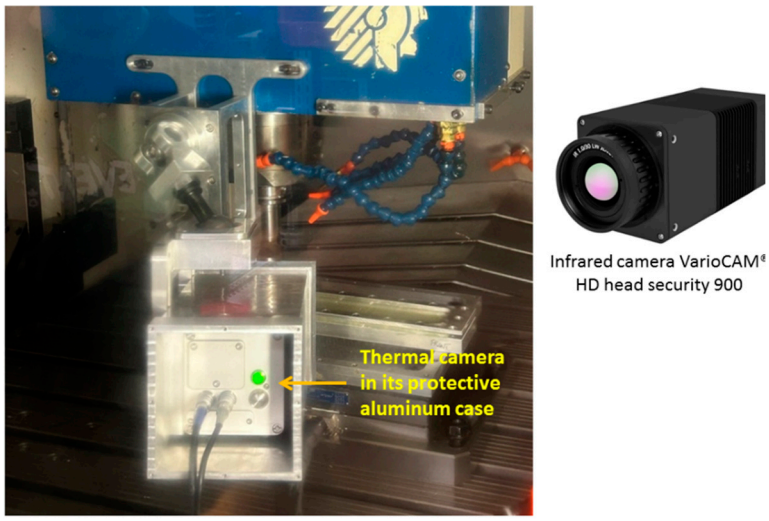

Figure 4. Experimental setup for monitoring temperature during the drilling process using the VarioCAM® HD head 900 infrared thermal camera.

2.2. Methods

A response surface regression approach was used to model drilling temperature as a function of spindle speed (S) and feed rate (F) across the different wax (W) and graphene (G) concentrations. For each concentration, a cubic response surface including linear, quadratic, interaction, and cubic terms was fitted by ordinary least squares:

$$\hat{Y} = \beta_0 + \beta_1 S + \beta_2 F + \beta_{11} S^2 + \beta_{12} SF + \beta_{22} F^2 + \beta_{111} S^3 + \beta_{112} S^2 F + \beta_{122} SF^2 + \beta_{222} F^3$$

A cubic model was chosen because preliminary analyses showed non-linear temperature trends at extreme speed/feed combinations that a quadratic model could not capture.

A dummy variable (D) framework was used to facilitate formal comparisons with the reference combination (W = 0%, G = 0%), allowing tests for intercept and slope differences between groups. Model adequacy was assessed via residual diagnostics, ANOVA of nested models, and fit statistics (R^2, adjusted R^2, RMSE, MAE, MAPE%, MPE%).

3. Results

The measured drilling temperatures across different experimental conditions reveal significant influences of feed rate, cutting speed, wax content, and graphene concentration on the thermal behavior of GFRP composites. These results are organized to examine the individual effects of feed rate and cutting speed under varying additive compositions.

3.1. Experimental Drilling Temperature Analysis

The study of machining temperatures is critically important, as excessive heat directly compromises tool life, dimensional accuracy, and surface finish, thereby affecting overall productivity. Accurate temperature measurement and rigorous modeling are essential to elucidate the complex thermal mechanisms in machining and to identify key influencing parameters, such as cutting speed and feed rate. This experimental study on drilling GFRP composites specifically investigates the relationships between feed rate, cutting speed, and temperature, analyzing how these interactions are modulated by variations in wax and graphene content.

3.1.1. Feed Rate Effects

At constant cutting speeds, increasing the feed rate from 0.02 to 0.08 mm/rev resulted in a non-monotonic variation in drilling temperature (Figures 5 and A1). For unmodified samples (0% wax, 0% graphene), temperature initially decreased with moderate feed increases before rising slightly at higher feeds. For example, at 50 mm/min, the mean temperature decreased from 73.6 °C at 0.02 mm/rev to 67.8 °C at 0.06 mm/rev and then increased to 69.8 °C at 0.08 mm/rev. This pattern, also observed with graphene-only additives, suggests moderate feed rates reduce tool–workpiece contact time, while higher feeds intensify mechanical deformation and localized heating.

The addition of wax significantly moderated this effect. With 2% wax and 0% graphene, temperature variation across feed rates diminished, exhibiting only minor fluctuations (e.g., 62.4–69.7 °C at 50 mm/min), indicating enhanced lubrication and thermal stability. Conversely, intermediate wax content (1%) combined with graphene (0.25–2%) generally produced higher temperatures at elevated feed rates. For instance, at 100 mm/min with 1% wax and 2% graphene, temperature increased from 67.5 °C to 69.1 °C, suggesting that specific additive combinations may exacerbate frictional heating or impede thermal transfer under aggressive machining conditions.

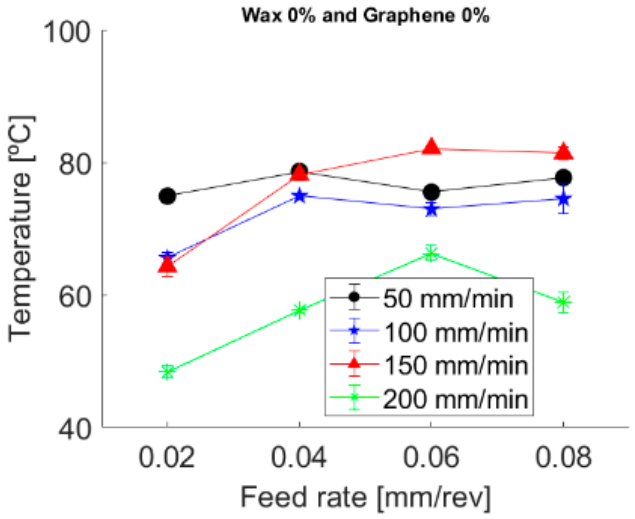

(**a**) 0% wax

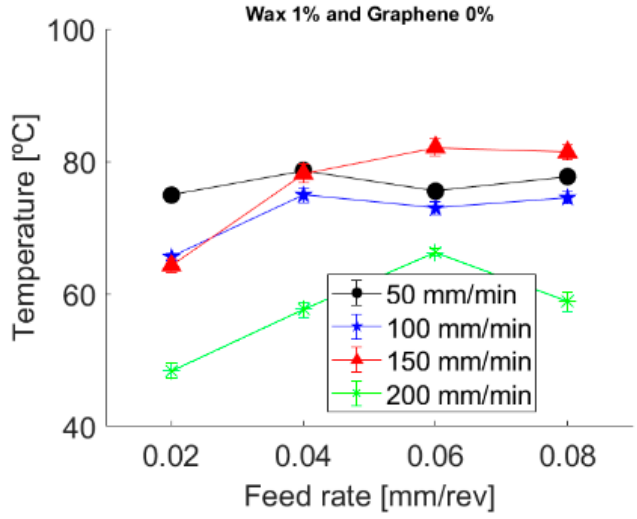

(**b**) 1% wax

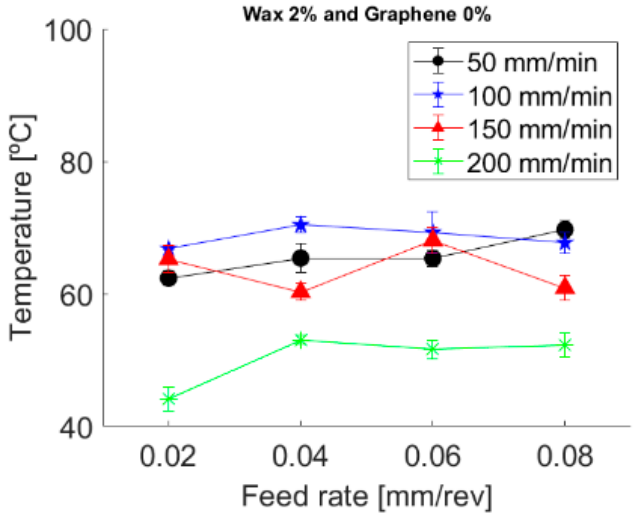

(**c**) 2% wax

Figure 5. Effect of feed rate on drilling temperatures at varying wax contents with 0% graphene.

3.1.2. Cutting Speed Effects

Increasing cutting speed generally reduced drilling temperatures, particularly in additive-free samples. At a 0.02 mm/rev feed with 0% wax and 0% graphene, the mean

temperature decreased from 73.6 °C at 50 mm/min to 65.2 °C at 200 mm/min. This trend, consistent across feed rates, suggests higher speeds limit thermal accumulation by reducing tool–workpiece contact time (Figures 6 and A2).

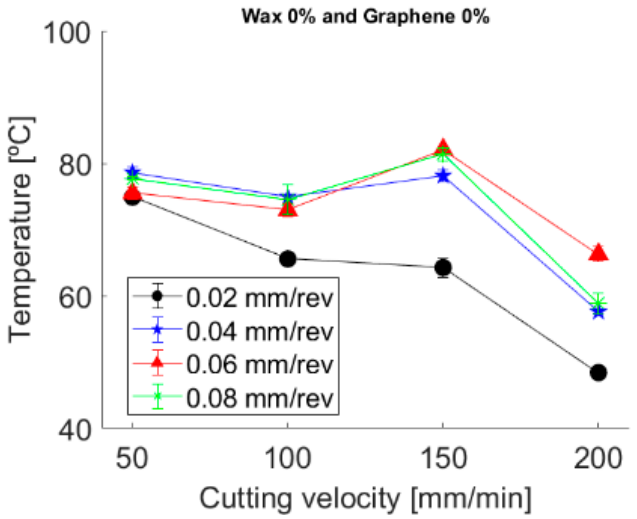

(**a**) 0% wax

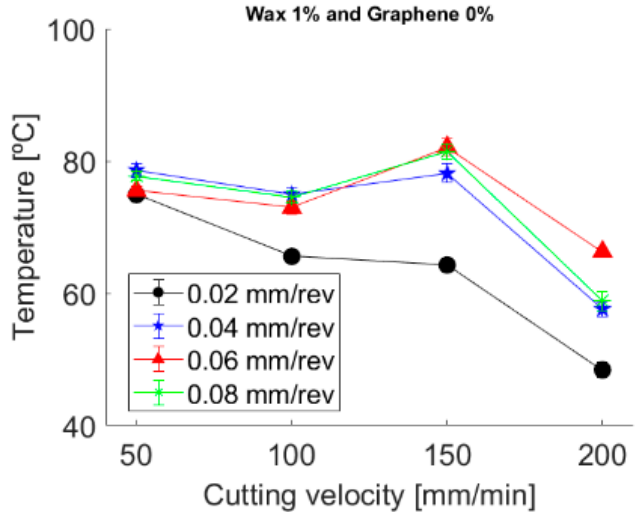

(**b**) 1% wax

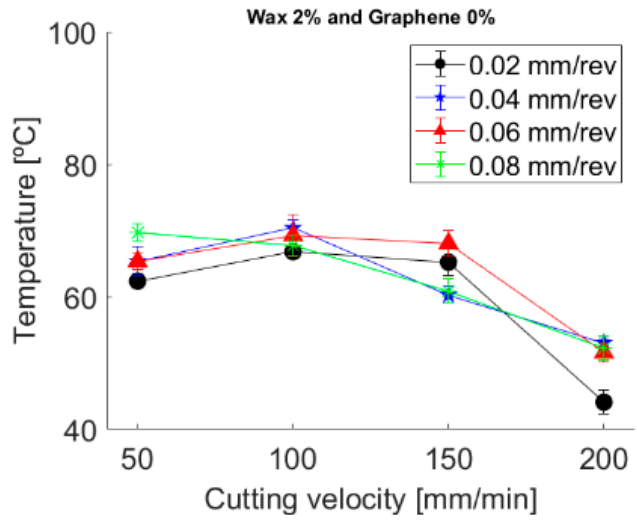

(**c**) 2% wax

Figure 6. Effect of cutting speed on drilling temperatures at varying wax contents with 0% graphene.

The temperature reduction was amplified with 2% wax. Under identical feed conditions (0.02 mm/rev), samples with 2% wax and 0% graphene exhibited a drop from 62.4 °C to 44.1 °C—the lowest temperature recorded—demonstrating a synergistic effect between high-speed cutting and wax lubrication.

In contrast, higher graphene concentrations disrupted this trend. With 2% graphene and 0% wax at 0.06 mm/rev, temperatures fluctuated between 72–81 °C without a clear decline, indicating that graphene agglomeration may impair thermal conductivity at elevated speeds, particularly without wax to aid dispersion.

3.2. Boxplot Analysis of Temperature Variation

(a) Effect of wax concentration

Wax content significantly influenced drilling temperatures (Figure 7a). Increasing wax from 0% to 2% reduced the median temperature from 69.77 °C to 66.13 °C, while the mean decreased from 68.72 °C to 64.64 °C. Temperature variability was highest without wax (IQR = 9.13 °C, SD = 7.36 °C) and decreased with 1% wax (IQR = 7.65 °C, SD = 6.28 °C). The minimum temperature consistently dropped with wax addition, reaching 44.1 °C at 2% wax.

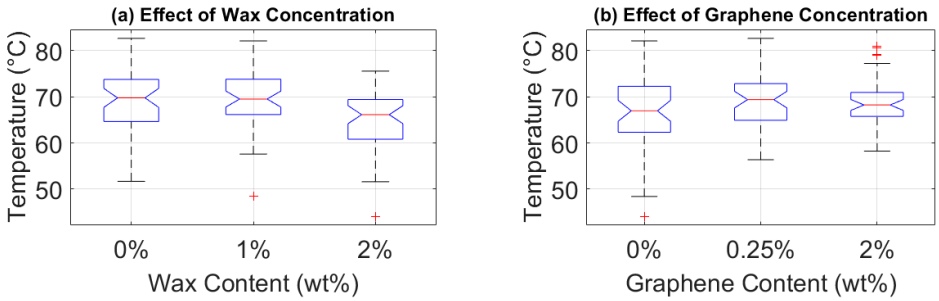

Figure 7. Boxplot analysis showing the effect of wax and graphene concentrations on temperature variation during drilling.

(b) Effect of graphene concentration

Graphene addition moderately increased temperatures but reduced variability (Figure 7b). The mean temperature rose from 66.32 °C (0% graphene) to 68.53 °C (2% graphene), while the standard deviation decreased from 8.60 °C to 5.53 °C. The interquartile range similarly contracted from 9.98 °C to 5.20 °C, indicating more stable thermal performance despite slightly elevated temperatures.

(c) Effect of feed rate

Higher feed rates produced systematically higher temperatures (Figure 8a). Mean temperature increased from 64.78 °C at 0.02 mm/rev to 69.51 °C at 0.08 mm/rev. Variability showed no clear trend, with the standard deviation ranging between 6.59–7.35 °C across feed rates. The temperature range expanded at intermediate feeds and then slightly contracted at the highest feed rate.

(d) Effect of Cutting Speed

Elevated cutting speeds substantially reduced drilling temperatures (Figure 8b). The mean temperature dropped from 70.52 °C at 50 mm/min to 60.39 °C at 200 mm/min. Variability initially increased with speed (SD = 3.68 °C at 50 mm/min to 7.08 °C at 150 mm/min) before stabilizing. The temperature range shifted downward at 200 mm/min (44.1–75.43 °C), confirming the cooling effect of high-speed machining.

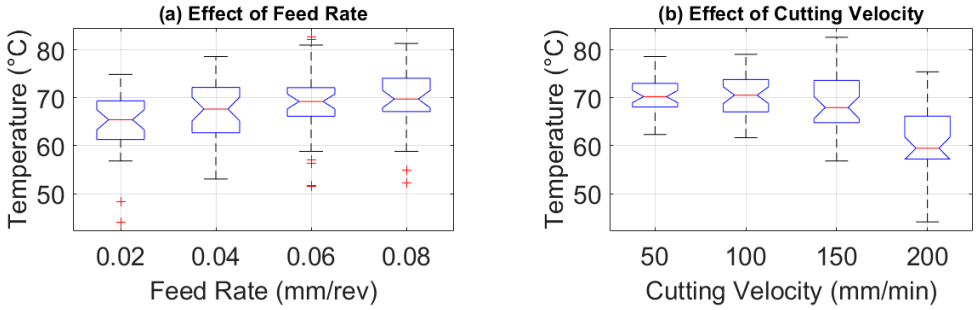

Figure 8. Boxplot analysis showing the effect of feed rate and cutting speed on temperature variation during drilling.

3.3. Effect of Wax and Graphene Combinations on Average Machining Temperature

Analysis of wax–graphene combinations reveals distinct thermal behavior patterns (Figure 9). The baseline case (0% wax, 0% graphene) exhibited a mean temperature of 66.32 °C. Introducing graphene without wax increased temperatures to 68.02 °C (0.25% graphene) and 68.53 °C (2% graphene), indicating graphene alone elevates thermal load.

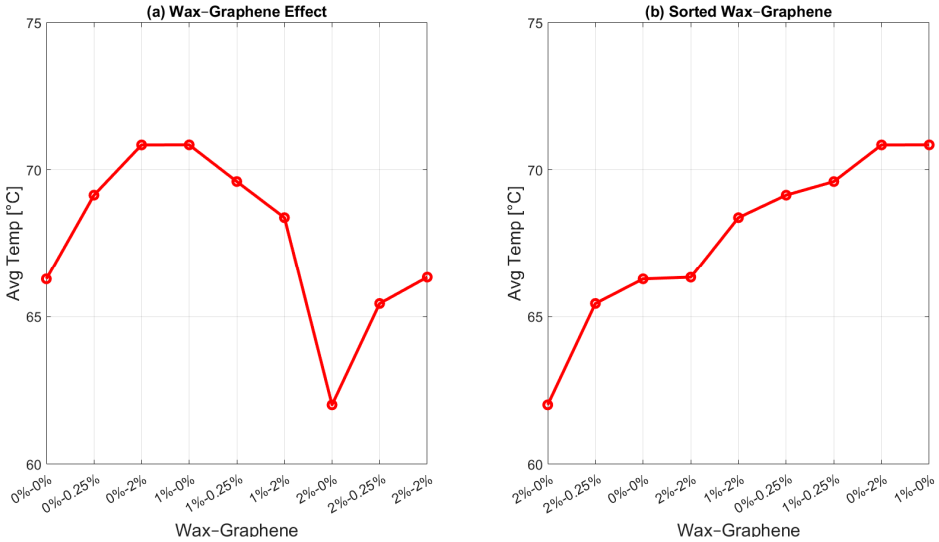

Figure 9. Evolution of mean temperature as a function of wax–graphene concentration, regardless of other parameters.

Wax concentration demonstrated a more substantial influence. While 1% wax showed minimal effect (69.50 °C), increasing to 2% wax significantly reduced the mean temperature to 64.64 °C. This cooling effect was accompanied by reduced variability, with standard deviation decreasing from 7.36 °C (0% wax) to approximately 6.3 °C with wax addition.

The combination data establish wax as the dominant factor in thermal regulation. The optimal condition (2% wax, 0% graphene) achieved the lowest temperature (64.64 °C), while the least favorable combination (1% wax, 0% graphene) produced the highest (69.50 °C). These results demonstrate that sufficient wax concentration effectively counteracts graphene's tendency to elevate machining temperatures.

3.4. Relative Contribution of Machining Parameters to Temperature Generation

Figure 10 illustrating the contributions of different machining parameters to the generated temperature. This visualization provides a clear view of the relative influence of each parameter during the machining process. The distribution reveals that cutting speed is by far the most dominant factor, accounting for 67.28% of the total temperature impact. In comparison, feed rate and wax concentration show nearly equal contributions,

representing 15.06% and 15.18% respectively. Lastly, graphene concentration contributes the least, with only 2.48% of the total impact on temperature.

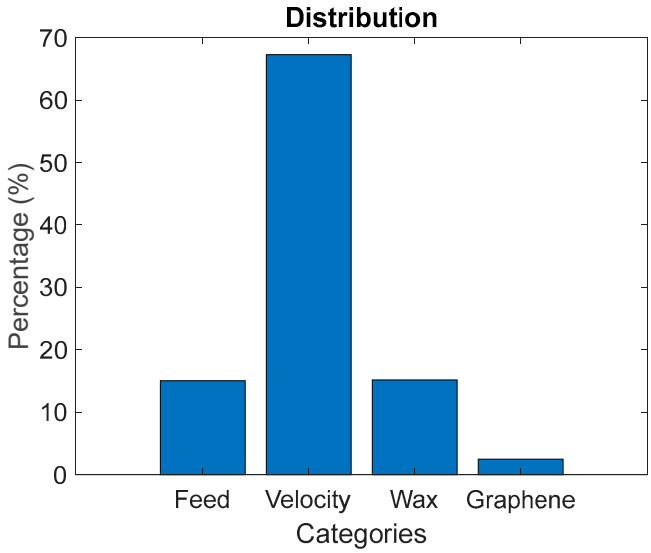

Figure 10. Contribution of machining parameters to generated temperature.

3.5. Prediction Results

The cubic models demonstrated excellent fit across all concentrations (Figure 11), with R^2 values ranging from 0.89 to 0.97 (Table 1). For the reference concentration (W = 0%, G = 0%), the estimated surface exhibited pronounced curvature in the high-speed regime (significant S^3 term). Non-reference concentrations showed systematic offsets from this baseline, with dummy variable tests revealing an average intercept shift of $\gamma = 1.24$ units across all modified compositions.

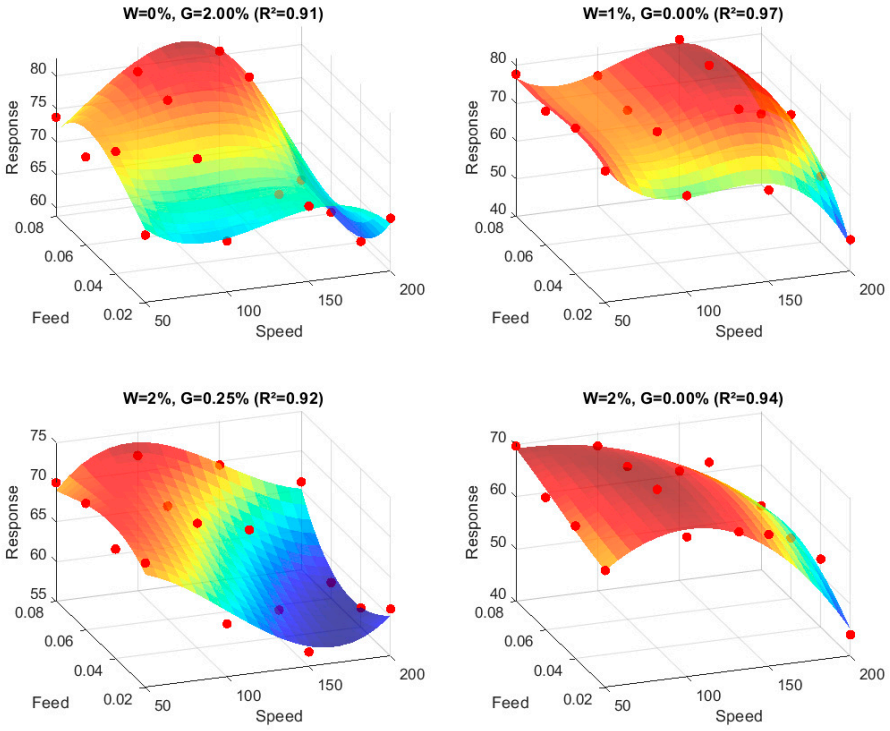

Figure 11. Prediction surfaces of drilling temperature and measured data.

Table 1. Goodness-of-fit statistics for response surface models by wax and graphene concentration.

W%	G%	R^2	Adj R^2	RMSE	MAE	MAPE%	Sample Size
0	0	0.90	0.88	2.87	1.51	2.28	16
0	0.25	0.90	0.88	3.01	1.58	2.38	16
0	2	0.92	0.91	2.60	1.58	2.16	16
1	0	0.97	0.94	2.52	1.34	2.01	16
1	0.25	0.91	0.89	2.56	1.35	2.03	16
1	2	0.89	0.87	3.60	1.89	2.86	16
2	0	0.94	0.93	3.03	1.44	2.37	16
2	0.25	0.92	0.90	2.58	1.26	1.92	16
2	2	0.90	0.88	3.08	1.62	2.44	16

Notably, three graphene-enhanced concentrations ($G \geq 0.5\%$) displayed additional slope shifts in feed rate sensitivity ($\delta F = -0.17$ to -0.23), suggesting altered material removal mechanics. Residual diagnostics, performed by analyzing the distribution of predicted versus measured values, confirmed the model's robustness. The absence of spatial patterns in the prediction errors (Figure 12) indicates a well-specified model. Data points aligned with the identity line (red) represent perfect predictions, while the proximity of all points to this line demonstrates minimal error between the model's forecasts and the actual observed values.

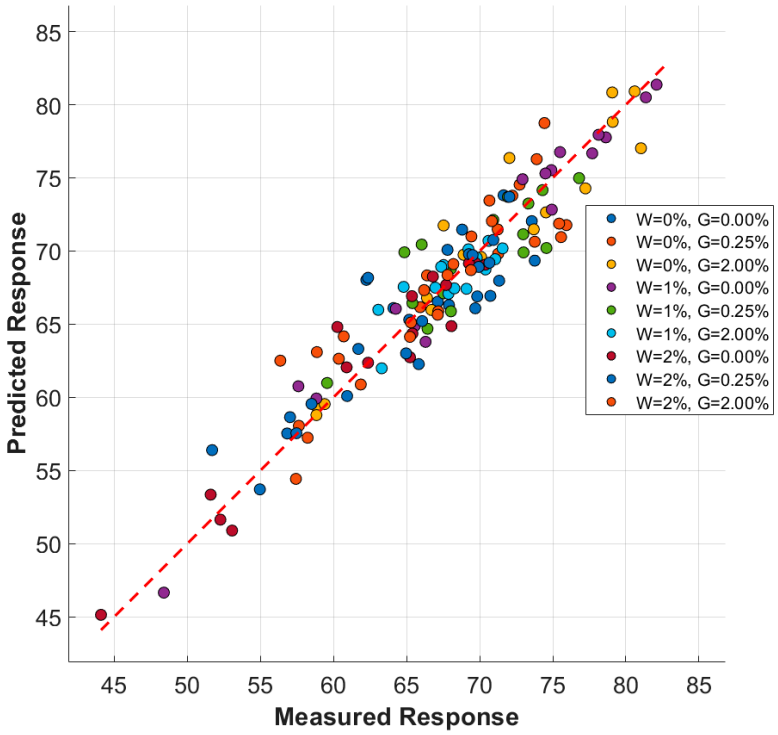

Figure 12. The distribution plot of predicted value and measured values.

The performance of the predictive models for drilling temperature, developed for various wax (W%) and graphene (G%) combinations, was evaluated using R^2 (coefficient of determination), adjusted R^2, root mean square error (RMSE), mean absolute error (MAE), and mean absolute percentage error (MAPE%). The results, based on a sample size of n = 16 for each combination, are comprehensively presented in Table 1.

The analysis reveals a significant influence of both additives on model accuracy. The highest explanatory power was achieved by the model for the 1% wax, 0% graphene (1%–0%) combination, yielding an R^2 of 0.97 and an adjusted R^2 of 0.94. This was accompanied by strong error metrics (RMSE = 2.52, MAE = 1.34, MAPE = 2.01%).

In terms of prediction precision, the 2% wax, 0.25% graphene (2%–0.25%) combination resulted in the lowest error values, with an MAE of 1.26 and a MAPE of 1.92%, indicating the most consistent and accurate forecasts, despite a slightly lower R^2 (0.92) than the best model.

Conversely, the control group without wax (0% wax, 0.25% graphene; W0 G0.25) exhibited the poorest performance among all combinations, with the highest RMSE (3.01) and among the highest MAE (1.58) and MAPE (2.38%) values.

4. Discussion

The use of additives, such as wax and graphene, plays a crucial role in reducing heat generated during machining. These additives act as lubricants and thermal dissipators, limiting heat accumulation at the cutting interface, as supported by Baldin et al. [47] for graphene-enriched minimum quantity lubrication and by Berman et al. [48] on graphene's solid-lubricant tribofilm behavior. Their benefit is concentration-dependent: too little yields weak lubrication, while too much can increase viscosity or induce agglomeration, compromising heat removal, consistent with dispersion/viscosity constraints reported for graphene additives by Shanmugapriyan et al. [4] and with additive-dependent tribology in cutting fluids shown by Ma et al. [49]. For wax, its role as a boundary solid lubricant (and latent-heat buffer when phase change is involved) is supported by Ameli Kalkhoran Lab's micro-machining study of wax-coated tools [50].

4.1. Interpretation of Drilling Temperature Trends

The complexity of feed-rate effects suggests that while moderate increases can reduce rubbing time and frictional heating, very high rates (e.g., 0.08 mm/rev) elevate temperatures due to excessive deformation and higher cutting forces, in agreement with the drilling-temperature review by Kalkhoran et al. [50]. The observation that the cooling/lubricating influence of 1% wax or 0.25% graphene can be counteracted at aggressive feeds aligns with reports that mechanical work and chip load can dominate over lubricant effects at high material-removal rates (in partial agreement with the additive-dependent performance trends summarized by Ma et al. [49].

Cutting-speed effects indicate a threshold for additive effectiveness. The reversal with 1% wax at 150 mm/min (peak ~82 °C) implies that above a certain speed, lubrication/cooling becomes effective, consistent with mechanisms noted by Zhu et al. [10], where higher speeds can shorten tool–workpiece contact time and improve chip evacuation, thereby reducing measured temperature in specific drilling regimes. Stabilization of temperature at ~2% graphene is in agreement with Baldin et al. [47], who reported optimal graphene loadings under MQL that balance improved heat transport/tribofilm formation against viscosity-driven penalties. The synergy of 1% wax + 0.25% graphene (optimal thermal stability across speeds) is supported by prior observations that boundary films plus thermally conductive nano-additives can act complementarily (Berman et al. [48]; Baldin et al. [47]).

Parameter interactions define operational zones: at low feeds/medium speeds (100–150 mm/min), heat generation rises without adequate lubrication, whereas higher speeds/feeds with additives reduce temperatures. Such speed × feed × coolant couplings are repeatedly reported in ANOVA/RSM studies of cutting temperature, with cutting speed typically dominant, in agreement with Zhu et al. [10] and consistent with multi-

factor analyses across machining operations. The observed low temperature (≈67 °C) and high stability (SD ≈1.2 °C) under 2% wax + 2% graphene at 200 mm/min and 0.08 mm/rev are therefore in line with operating in a high-speed, assisted-cooling zone described in the literature.

4.2. Boxplot Analysis

Wax concentration shows minimal change in medians, while graphene slightly raises the median but reduces variability at higher loading (IQR shrinkage). This pattern—higher uniformity due to better heat spreading/tribofilm stability despite modest mean-temperature shifts—is in agreement with graphene-additive tribology summaries (Berman et al. [48]) and with MQL machining experiments that emphasize stability/consistency improvements at suitable graphene dosages (Baldin et al. [47]). The modest positive correlation between feed and temperature but persistent scatter agrees with the broad variability sources (chip evacuation, local heterogeneity) emphasized in the drilling-temperature review of Zhu et al. [10].

4.3. Implications of Parameter Influence for Thermal Control and Process Optimization

Cutting speed is the dominant factor, in agreement Zhu et al. [10]. Feed and wax act as secondary levers for thermal control. The small direct contribution of graphene concentration (~2–3%) to mean temperature aligns with machining reports where graphene's main benefit is friction reduction and thermal stability rather than large mean reductions at every setting (Baldin et al. [47]; Berman et al. [48]). Accordingly, it is important to prioritize precise speed control while adjusting feed and additive levels, which is consistent with prior findings.

4.4. Thermal Behavior and Uncertainty Associated with Wax Concentration

The results clearly demonstrate that wax concentration plays a critical role in controlling drilling temperatures. The most substantial cooling effect was observed at 2% wax, where both mean and median temperatures were significantly lower compared to 0% and 1% concentrations. This suggests that wax becomes more effective at higher concentrations, potentially due to enhanced lubrication and improved heat dissipation during drilling [50].

While 2% wax showed the greatest reduction in temperature, the 1% concentration offered the narrowest distribution and lowest variability, pointing to superior process stability. This indicates that while higher wax concentrations maximize cooling efficiency, lower concentrations may be advantageous where consistency and repeatability are prioritized [10].

The progressive reduction in minimum temperature across all wax levels provides strong evidence of wax's cooling influence under demanding cutting conditions. This behavior highlights a concentration-dependent mechanism, where increasing wax content enhances its thermal management capability.

Taken together, these findings suggest that 2% wax concentration offers the most effective balance for thermal control in drilling of GFRP materials. It delivers significant reductions in average and median temperatures while maintaining acceptable variability. For applications that require both stability and effective cooling, the results recommend 2% wax as the optimal concentration.

4.5. Thermal Effects and Uncertainty Linked to Graphene Concentration

Graphene addition moderately increased mean drilling temperatures relative to the additive-free condition, suggesting additional frictional resistance at the tool–workpiece interface. However, its primary effect was a substantial reduction in thermal variability. The

interquartile range decreased from 9.98 °C (0% graphene) to 5.20 °C (2% graphene), while standard deviation similarly declined, indicating significantly stabilized thermal behavior.

This stabilization is reflected in the narrowed temperature distribution, where increased minimum temperatures combined with slightly reduced maximum values produced a tighter operational range. The observed behavior aligns with established tribological mechanisms [48] and concentration-dependent dispersion effects [51] and with graphene's tribological mechanisms [48], where enhanced heat spreading and boundary-film stability occur alongside increased viscosity or shear heating.

While graphene elevates average temperatures, the enhanced thermal stability at 2% concentration provides critical process reliability benefits, particularly in applications requiring uniform heat distribution to prevent localized damage and preserve material integrity.

4.6. Combined Effects of Wax and Graphene on Thermal Management

Across our trials, wax dominated the reduction in absolute drilling temperature, while graphene's contribution was subtler—its addition tended to keep means roughly the same or slightly higher, but it tightened the spread (lower IQR/Std) and improved thermal uniformity. When used together, wax suppressed peak temperatures and graphene helped distribute heat and maintain a stable cutting interface, yielding cooler and more consistent temperature profiles than graphene alone. This division of roles—wax for boundary-film cooling and graphene for heat spreading/low-shear interfacial sliding—is consistent with the tribological literature (Berman et al. [48]; Baldin et al. [47], Gheisari et al. [52])

Mechanistically, paraffin wax acts as a boundary-film/phase-change additive: it can form protective, low-shear surface layers and buffer transient heat spikes by absorbing/releasing latent heat. Recent work on microencapsulated paraffin in polymeric coatings reports exceptionally low friction and wear, highlighting the ability of wax-based additives to stabilize contact and manage heat under load [52].

Although graphene additives are widely recognized for improving thermal conductivity in polymer-based composites [40,41], and wax functions as a solid lubricant that minimizes frictional heating during machining [17], their combined influence on temperature control arises from distinct mechanisms. Wax mainly reduces friction and dissipates surface heat through lubrication and latent heat absorption, whereas graphene enhances internal heat conduction within the matrix. However, graphene's practical thermal efficiency can be hindered by agglomeration and poor interfacial bonding at higher loadings, which disrupts uniform heat transfer. As a result, while graphene offers theoretical thermal advantages, these may be offset by dispersion challenges, explaining the slightly elevated mean temperatures compared to wax-enriched composites.

Crucially, there is direct evidence that combining graphene oxide with paraffin wax yields synergistic tribological benefits—lower friction and wear than either component alone—due to a robust tribofilm formed by the hybrid system. This aligns with our observation that adding wax alongside graphene mitigates graphene's slight mean-temperature increase while preserving graphene's uniformity gains. Graphene's role is well documented: few-layer graphene and graphene platelets can form low-shear transfer films and spread heat laterally, reducing interfacial resistance and smoothing temperature transients. Foundational studies show graphene functioning as a solid lubricant/coating that lowers friction and wear, and as a dispersed oil additive after surface modification to improve stability mechanisms that explain the improved temperature consistency observed even when mean temperatures are not strongly reduced by graphene alone [48,53].

4.7. Feed Rate Influence and Associated Variability

The results clearly demonstrate that increasing feed rate leads to higher drilling temperatures. Both mean and median values progressively rise from 0.02 mm/rev to 0.08 mm/rev, reflecting greater frictional heating and higher energy input as material removal rates increase (Figure 8a). This trend is consistent with the expectation that higher feed rates impose greater cutting forces, which in turn generate more heat at the tool–workpiece interface [10].

In terms of consistency, the narrowest IQR occurred at 0.06 mm/rev, suggesting relatively uniform behavior despite elevated temperatures. At the highest feed (0.08 mm/rev), variability remained moderate, whereas the lowest feed (0.02 mm/rev) produced both lower averages and wider spreads.

Overall, raising feed rate improves material removal efficiency but intensifies thermal loading. The results highlight a trade-off: higher productivity at the expense of increased and more uniformly high drilling temperatures, which may affect tool life and hole quality.

4.8. Cutting Speed as a Key Thermal Management Parameter

Cutting speed played a critical role in thermal behavior during drilling. At 50–150 mm/min, mean and median temperatures remained relatively stable. However, a marked drop occurred at 200 mm/min, with both averages falling significantly. This suggests that very high cutting speeds can reduce heat accumulation, likely due to reduced contact duration and more efficient chip evacuation. Studies on drilling GFRP and other composites have similarly noted that higher cutting speeds can lead to lower temperatures, particularly when paired with optimized feeds or tool geometries [54,55].

Temperature variability increased alongside cutting speed—peaking at 150 mm/min—before stabilizing slightly at 200 mm/min. This pattern indicates that while elevated speeds reduce overall thermal levels, they may introduce localized fluctuations, possibly due to intermittent contact or thermal cycling. It aligns with observations that higher speeds improve cooling but may exacerbate non-uniform heating unless adequately controlled [54].

Moreover, the range analysis shows both minimum and maximum temperatures were lower at 200 mm/min than at intermediate speeds. This points to improved thermal control at extreme velocities—a finding consistent with the notion that higher speeds can confine heat within the chip and away from the cutting zone, benefiting tool life and hole quality [54,55].

In essence, cutting speed exhibits a dual effect: lower speeds support thermal stability, whereas very high speeds deliver superior cooling. This underscores the need to balance thermal management with process consistency when optimizing drilling parameters.

4.9. Model Performance Analysis

The predictive models reveal complex wax–graphene interactions in thermal regulation during drilling. The 1% wax, 0% graphene (W1 G0) model demonstrated exceptional explanatory power ($R^2 = 0.97$), indicating highly predictable thermal behavior with moderate wax addition.

However, the 2% wax, 0.25% graphene (W2 G0.25) combination achieved superior precision with the lowest errors (MAE = 1.26, MAPE = 1.92%), suggesting that this specific formulation minimizes random variability despite graphene's limited contribution to model structure.

The critical importance of wax is evident from the consistently poor performance of wax-free combinations (e.g., W0 G0.25: RMSE = 3.01, MAPE = 2.38%), which exhibited greater thermal instability. Conversely, the 1% wax, 2% graphene (W1 G2) combination yielded the highest errors among wax-containing samples (RMSE = 3.60, MAPE = 2.86%),

indicating detrimental interaction effects potentially due to graphene agglomeration or disrupted thermal transfer mechanisms at intermediate wax concentrations.

5. Conclusions

This study systematically investigated the influence of graphene and wax additives on the thermal behavior of GFRP composites during drilling. Based on the experimental findings and predictive modeling, the following conclusions can be drawn:

- The thermal response of GFRP composites is strongly governed by additive concentration and its interaction with drilling parameters.
- A 2% wax formulation without graphene proved most effective in reducing average drilling temperature, confirming wax's role as a boundary lubricant and thermal buffer.
- Graphene alone slightly increased average drilling temperatures but significantly reduced thermal variability, contributing to a more stable machining process.
- Cutting speed was identified as the dominant factor, with higher speeds (200 mm/min) lowering temperatures due to reduced tool–workpiece contact time.
- The developed cubic response surface models (R^2 = 0.89–0.97) demonstrated high predictive capability, offering a reliable tool for forecasting thermal behavior and optimizing machining strategies.

While 2% wax demonstrated the most effective thermal reduction at high cutting speeds, its use involves practical trade-offs. The presence of residual wax may necessitate post-machining cleaning to maintain surface quality, and excessive wax incorporation could slightly affect the composite's mechanical integrity or fiber–matrix adhesion. Nevertheless, when properly controlled, wax remains a practical and efficient thermal-management additive for improving drilling performance in GFRP composites.

Author Contributions: Conceptualization, M.S. and J.-F.C.; methodology, M.S. and S.J.; software, M.S.; validation, M.S. and J.-F.C.; formal analysis, M.S.; investigation, M.S.; resources, J.-F.C.; data curation, S.J.; writing—original draft preparation, M.S.; writing—review and editing, M.S. and J.-F.C.; visualization, M.S.; supervision, J.-F.C.; project administration, J.-F.C.; funding acquisition, J.-F.C. All authors have read and agreed to the published version of the manuscript.

Funding: This research was funded by the Natural Sciences and Engineering Research Council of Canada (NSERC) grant number RGPIN-2017-04305.

Data Availability Statement: The original contributions presented in this study are included in the article. Further inquiries can be directed to the corresponding author.

Acknowledgments: The authors gratefully acknowledge the financial support of the Natural Sciences and Engineering Research Council of Canada (NSERC).

Conflicts of Interest: The authors declare no conflicts of interest. The funders had no role in the design of the study; in the collection, analyses, or interpretation of data; in the writing of the manuscript; or in the decision to publish the results.

Abbreviations

The following abbreviations are used in this manuscript:

RSM	Response Surface Methodology
PCM	Phase Change Material
SD	Standard Deviation
IQR	Interquartile Range
ANOVA	Analysis of Variance
GFRP	Glass Fiber Reinforced Polymer
CNC	Computer Numerical Control

Appendix A

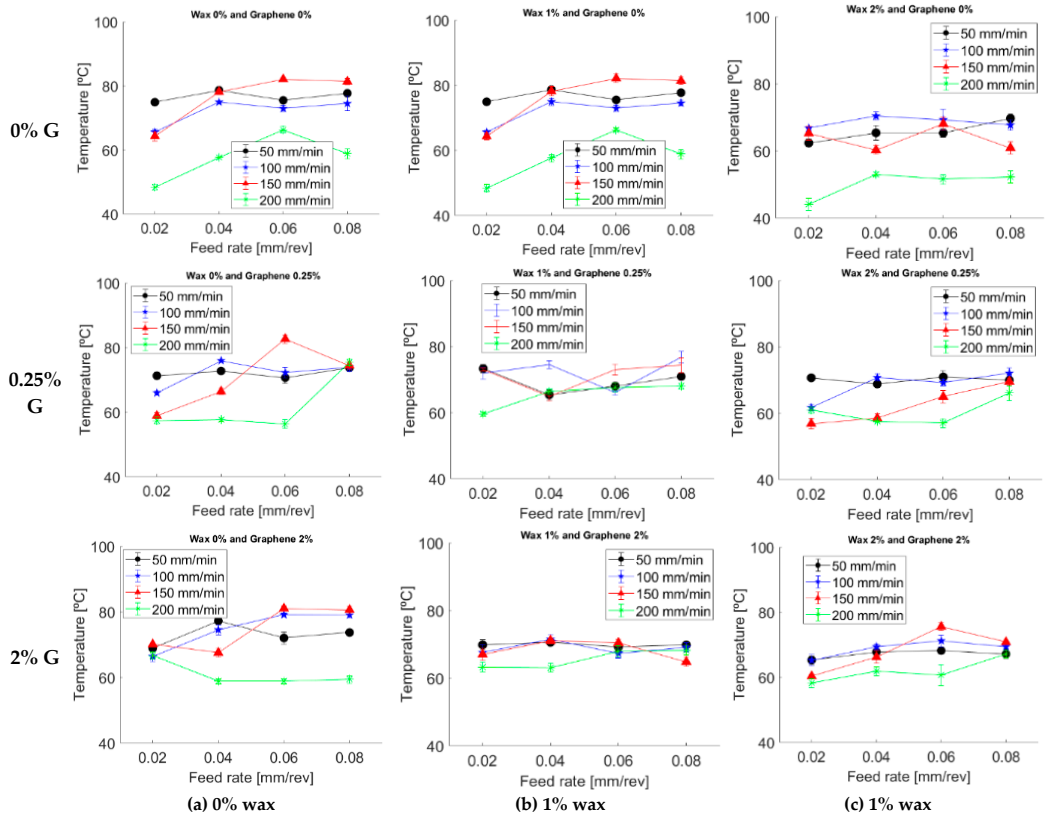

Figure A1. Feed rate effect on drilling temperatures at varying wax and graphene levels.

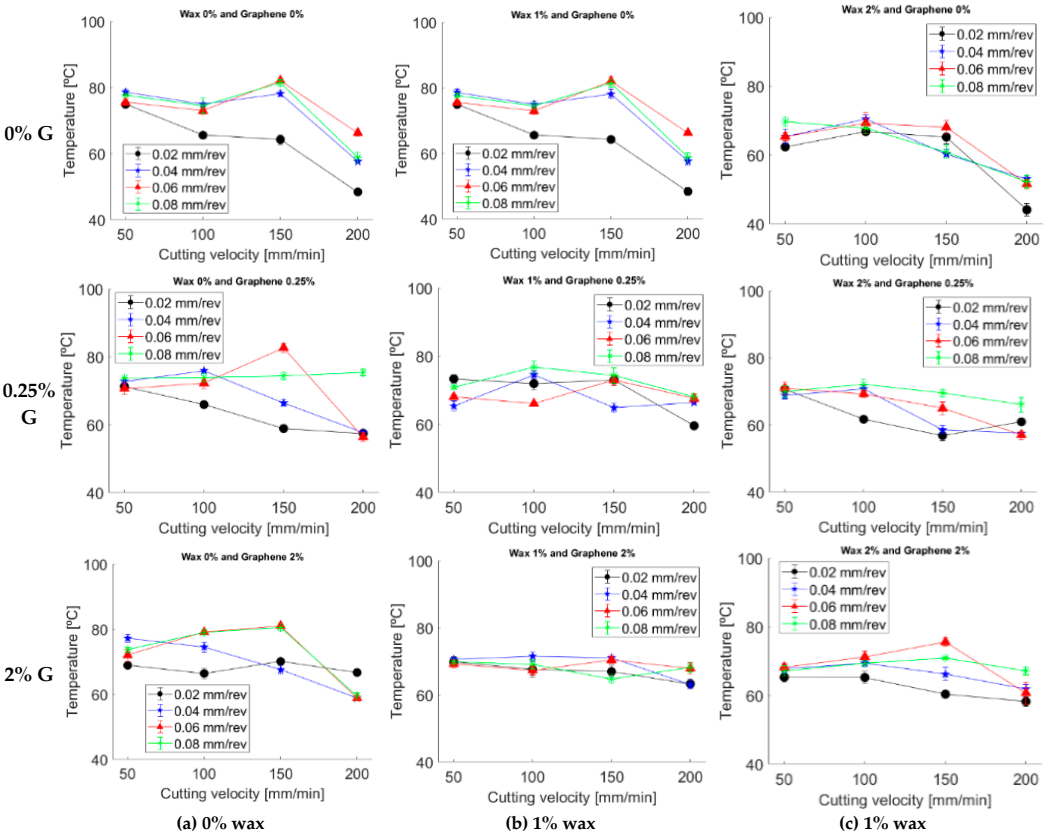

Figure A2. Cutting speed effect on drilling temperatures at varying wax and graphene levels.

References

1. Malik, K.; Ahmad, F.; Keong, W.T.; Gunister, E. The effects of drilling parameters on thrust force, temperature and hole quality of glass fiber reinforced polymer composites. *Polym. Polym. Compos.* **2022**, *30*, 09673911221131113. [CrossRef]
2. Reyhan, R.R.; Andoko, A.; Prasetya, R. The Effect of Feed Rate Variation and Cooling on the Drilling Process of Carbon Fiber and Glass Fiber Composites. *J. Appl. Sci. Eng. Technol. Educ.* **2024**, *6*, 118–126. [CrossRef]
3. Slamani, M.; Chatelain, J.-F. Kriging versus Bezier and regression methods for modeling and prediction of cutting force and surface roughness during high speed edge trimming of carbon fiber reinforced polymers. *Measurement* **2020**, *152*, 107370. [CrossRef]
4. Slamani, M.; Chafai, H.; Chatelain, J. Effect of milling parameters on the surface quality of a flax fiber-reinforced polymer composite. *Proc. Inst. Mech. Eng. Part E J. Process Mech. Eng.* **2024**, *238*, 1537–1544. [CrossRef]
5. Mudegowdar, M. Influence of cutting parameters during drilling of filled glass fabric-reinforced epoxy composites. *Sci. Eng. Compos. Mater.* **2015**, *22*, 81–88. [CrossRef]
6. Jessy, K.; Satish Kumar, S.; Dinakaran, D.; Seshagiri Rao, V. Influence of different cooling methods on drill temperature in drilling GFRP. *Int. J. Adv. Manuf. Technol.* **2015**, *76*, 609–621. [CrossRef]
7. Biruk-Urban, K.; Bere, P.; Udroiu, R.; Józwik, J.; Beer-Lech, K. Understanding the Effect of Drilling Parameters on Hole Quality of Fiber-Reinforced Polymer Structures. *Polymers* **2024**, *16*, 2370. [CrossRef]
8. Tian, J.; Wu, F.; Zhang, P.; Lin, B.; Liu, T.; Liu, L. The coupling effect and damage analysis when drilling GFRP laminates using candlestick drills. *Int. J. Adv. Manuf. Technol.* **2019**, *102*, 519–531. [CrossRef]
9. Thangavel, A.; Kuppusamy, R.; Lakshmanan, R. Optimization of drilling parameters using GRA for polyamide 6 nanocomposites. *Matéria* **2023**, *28*, e20220337. [CrossRef]
10. Zhu, Z.; Sun, X.; Guo, K.; Sun, J.; Li, J. Recent advances in drilling tool temperature: A state-of-the-art review. *Chin. J. Mech. Eng.* **2022**, *35*, 148. [CrossRef]
11. Franz, G.; Vantomme, P.; Hassan, M.H. A review on drilling of multilayer fiber-reinforced polymer composites and aluminum stacks: Optimization of strategies for improving the drilling performance of aerospace assemblies. *Fibers* **2022**, *10*, 78. [CrossRef]
12. Spanu, P.; Abaza, B.F.; Constantinescu, T.C. Analysis and Prediction of Temperature Using an Artificial Neural Network Model for Milling Glass Fiber Reinforced Polymer Composites. *Polymers* **2024**, *16*, 3283. [CrossRef]
13. Biruk-Urban, K.; Bere, P.; Józwik, J. Machine learning models in drilling of different types of glass-fiber-reinforced polymer composites. *Polymers* **2023**, *15*, 4609. [CrossRef]
14. Pereira, O.; Rodríguez, A.; Barreiro, J.; Fernández-Abia, A.I.; de Lacalle, L.N.L. Nozzle design for combined use of MQL and cryogenic gas in machining. *Int. J. Precis. Eng. Manuf. -Green Technol.* **2017**, *4*, 87–95. [CrossRef]
15. Pereira, O.; Català, P.; Rodríguez, A.; Ostra, T.; Vivancos, J.; Rivero, A.; López-de-Lacalle, L.N. The use of hybrid CO_2+ MQL in machining operations. *Procedia Eng.* **2015**, *132*, 492–499. [CrossRef]
16. Pereira, O.; Celaya, A.; Urbikaín, G.; Rodríguez, A.; Fernández-Valdivielso, A.; de Lacalle, L.N.L. CO_2 cryogenic milling of Inconel 718: Cutting forces and tool wear. *J. Mater. Res. Technol.* **2020**, *9*, 8459–8468. [CrossRef]
17. Rao, Y.S.; Mohan, N.S.; Shetty, N.; Acharya, S. Drilling response of carbon fabric/solid lubricant filler/epoxy hybrid composites: An experimental investigation. *J. Compos. Sci.* **2023**, *7*, 46. [CrossRef]
18. Kargar, F.; Barani, Z.; Salgado, R.; Debnath, B.; Lewis, J.S.; Aytan, E.; Lake, R.K.; Balandin, A.A. Thermal percolation threshold and thermal properties of composites with high loading of graphene and boron nitride fillers. *ACS Appl. Mater. Interfaces* **2018**, *10*, 37555–37565. [CrossRef]
19. Danayat, S.; Nayal, A.S.; Tarannum, F.; Annam, R.; Muthaiah, R.; Arulanandam, M.K.; Garg, J. Superior enhancement in thermal conductivity of epoxy/graphene nanocomposites through use of dimethylformamide (DMF) relative to acetone as solvent. *MethodsX* **2023**, *11*, 102319. [CrossRef]
20. Lewis, J.S.; Barani, Z.; Magana, A.S.; Kargar, F.; Balandin, A.A. Thermal and Electrical Properties of Hybrid Composites with Graphene and Boron Nitride Fillers. *arXiv* **2019**, arXiv:1903.01025.
21. Unal, E. Temperature and thrust force analysis on drilling of glass fiber reinforced plastics. *Therm. Sci.* **2019**, *23*, 347–352. [CrossRef]
22. Xu, J.; Li, C.; El Mansori, M.; Liu, G.; Chen, M. Study on the frictional heat at tool-work interface when drilling CFRP composites. *Procedia Manuf.* **2018**, *26*, 415–423. [CrossRef]
23. Zitoune, R.; Cadorin, N.; Collombet, F.; Šíma, M. Temperature and wear analysis in function of the cutting tool coating when drilling of composite structure: In situ measurement by optical fiber. *Wear* **2017**, *376*, 1849–1858. [CrossRef]
24. Nightingale, C.; Day, R. Flexural and interlaminar shear strength properties of carbon fibre/epoxy composites cured thermally and with microwave radiation. *Compos. Part A Appl. Sci. Manuf.* **2002**, *33*, 1021–1030. [CrossRef]
25. Gao, C.; Xiao, J.; Xu, J.; Ke, Y. Factor analysis of machining parameters of fiber-reinforced polymer composites based on finite element simulation with experimental investigation. *Int. J. Adv. Manuf. Technol.* **2016**, *83*, 1113–1125. [CrossRef]
26. Hocheng, H.; Tsao, C. Comprehensive analysis of delamination in drilling of composite materials with various drill bits. *J. Mater. Process. Technol.* **2003**, *140*, 335–339. [CrossRef]

27. Gaitonde, V.; Karnik, S.; Rubio, J.C.; Correia, A.E.; Abrão, A.; Davim, J.P. Analysis of parametric influence on delamination in high-speed drilling of carbon fiber reinforced plastic composites. *J. Mater. Process. Technol.* **2008**, *203*, 431–438. [CrossRef]
28. Sorrentino, L.; Turchetta, S.; Bellini, C. In process monitoring of cutting temperature during the drilling of FRP laminate. *Compos. Struct.* **2017**, *168*, 549–561. [CrossRef]
29. Chen, W.-C. Some experimental investigations in the drilling of carbon fiber-reinforced plastic (CFRP) composite laminates. *Int. J. Mach. Tools Manuf.* **1997**, *37*, 1097–1108. [CrossRef]
30. Rawat, S.; Attia, H. Wear mechanisms and tool life management of WC–Co drills during dry high speed drilling of woven carbon fibre composites. *Wear* **2009**, *267*, 1022–1030. [CrossRef]
31. Meshreki, M.; Damir, A.; Sadek, A.; Attia, M. Investigation of drilling of CFRP-aluminum stacks under different cooling modes. In Proceedings of the ASME International Mechanical Engineering Congress and Exposition, Phoenix, AZ, USA, 11–17 November 2016; American Society of Mechanical Engineers: New York, NY, USA, 2016.
32. Giasin, K.; Ayvar-Soberanis, S.; Hodzic, A. The effects of minimum quantity lubrication and cryogenic liquid nitrogen cooling on drilled hole quality in GLARE fibre metal laminates. *Mater. Des.* **2016**, *89*, 996–1006. [CrossRef]
33. Renteria, J.; Legedza, S.; Salgado, R.; Balandin, M.; Ramirez, S.; Saadah, M.; Kargar, F.; Balandin, A. Magnetically-functionalized self-aligning graphene fillers for high-efficiency thermal management applications. *Mater. Des.* **2015**, *88*, 214–221. [CrossRef]
34. Shahil, K.M.; Balandin, A.A. Graphene—Multilayer graphene nanocomposites as highly efficient thermal interface materials. *Nano Lett.* **2012**, *12*, 861–867. [CrossRef]
35. Gulotty, R.; Castellino, M.; Jagdale, P.; Tagliaferro, A.; Balandin, A.A. Effects of functionalization on thermal properties of single-wall and multi-wall carbon nanotube–polymer nanocomposites. *ACS Nano* **2013**, *7*, 5114–5121. [CrossRef]
36. Xian, G.; Qi, X.; Shi, J.; Tian, J.; Xiao, H. Toughened and self-healing carbon nanotube/epoxy resin composites modified with polycaprolactone filler for coatings, adhesives and FRP. *J. Build. Eng.* **2025**, *111*, 113207. [CrossRef]
37. Barani, Z.; Mohammadzadeh, A.; Geremew, A.; Huang, C.Y.; Coleman, D.; Mangolini, L.; Kargar, F.; Balandin, A.A. Thermal properties of the binary-filler hybrid composites with graphene and copper nanoparticles. *Adv. Funct. Mater.* **2020**, *30*, 1904008. [CrossRef]
38. El-Ghaoui, K.; Chatelain, J.-F.; Ouellet-Plamondon, C. Effect of graphene on machinability of glass fiber reinforced polymer (GFRP). *J. Manuf. Mater. Process.* **2019**, *3*, 78. [CrossRef]
39. Palanikumar, K.; Latha, B.; Senthilkumar, V.; Davim, J.P. Analysis on drilling of glass fiber–reinforced polymer (GFRP) composites using grey relational analysis. *Mater. Manuf. Process.* **2012**, *27*, 297–305. [CrossRef]
40. Li, A.; Zhang, C.; Zhang, Y.-F. Thermal conductivity of graphene-polymer composites: Mechanisms, properties, and applications. *Polymers* **2017**, *9*, 437. [CrossRef]
41. Liu, L.; Xu, C.; Yang, Y.; Fu, C.; Ma, F.; Zeng, Z.; Wang, G. Graphene-based polymer composites in thermal management: Materials, structures and applications. *Mater. Horiz.* **2025**, *12*, 64–91. [CrossRef]
42. Donaldson, K.; Stone, V.; Tran, C.; Kreyling, W.; Borm, P.J. Nanotoxicology. *Occup. Environ. Med.* **2004**, *61*, 727–728. [CrossRef]
43. Shvedova, A.; Kisin, E.; Porter, D.; Schulte, P.; Kagan, V.; Fadeel, B.; Castranova, V. Mechanisms of pulmonary toxicity and medical applications of carbon nanotubes: Two faces of Janus? *Pharmacol. Ther.* **2009**, *121*, 192–204. [CrossRef]
44. OECD. *Strategies, Techniques and Sampling Protocols for Determining the Concentrations of Manufactured Nanomaterials in Air at the Workplace*; OECD Publishing: Paris, France, 2017.
45. Rafiee, M.A.; Rafiee, J.; Wang, Z.; Song, H.; Yu, Z.-Z.; Koratkar, N. Enhanced mechanical properties of nanocomposites at low graphene content. *ACS Nano* **2009**, *3*, 3884–3890. [CrossRef]
46. Cui, Y.; Wang, G.; Wang, W.; Cui, X.; Dong, W.; Wang, C.; Jin, M.; He, T.; Zhang, Z.; Liu, L. Trade-off between interface stiffening and Young's modulus weakening in graphene/PMMA nanocomposites. *Compos. Sci. Technol.* **2022**, *225*, 109483. [CrossRef]
47. Baldin, V.; Rosa Ribeiro da Silva, L.; Houck, C.F.; Gelamo, R.V.; Machado, Á.R. Effect of graphene addition in cutting fluids applied by MQL in end milling of AISI 1045 steel. *Lubricants* **2021**, *9*, 70. [CrossRef]
48. Berman, D.; Erdemir, A.; Sumant, A.V. Graphene: A new emerging lubricant. *Mater. Today* **2014**, *17*, 31–42. [CrossRef]
49. Ma, J.; Gali, O.A.; Riahi, R.A. An evaluation of the tribological behavior of cutting fluid additives on aluminum-manganese alloys. *Lubricants* **2021**, *9*, 84. [CrossRef]
50. Ameli Kalkhoran, S.N.; Vahdati, M.; Zhang, Z.; Yan, J. Influence of wax lubrication on cutting performance of single-crystal silicon in ultraprecision microgrooving. *Int. J. Precis. Eng. Manuf. -Green Technol.* **2021**, *8*, 611–624. [CrossRef]
51. Liu, Y.; Yu, S.; Shi, Q.; Ge, X.; Wang, W. Graphene-family lubricant additives: Recent developments and future perspectives. *Lubricants* **2022**, *10*, 215. [CrossRef]
52. Gheisari, R.; Vazquez, M.; Tsigkis, V.; Erdemir, A.; Wooley, K.L.; Polycarpou, A.A. Microencapsulated paraffin as a tribological additive for advanced polymeric coatings. *Friction* **2023**, *11*, 1939–1952. [CrossRef]
53. Berman, D.; Erdemir, A.; Sumant, A.V. Graphene as a protective coating and superior lubricant for electrical contacts. *Appl. Phys. Lett.* **2014**, *105*, 231907. [CrossRef]

54. Khashaba, U.A.; Abd-Elwahed, M.S.; Eltaher, M.A.; Najjar, I.; Melaibari, A.; Ahmed, K.I. Thermo-mechanical and delamination properties in drilling GFRP composites by various drill angles. *Polymers* **2021**, *13*, 1884. [CrossRef] [PubMed]
55. Erturk, A.T.; Vatansever, F.; Yarar, E.; Guven, E.A.; Sinmazcelik, T. Effects of cutting temperature and process optimization in drilling of GFRP composites. *J. Compos. Mater.* **2021**, *55*, 235–249. [CrossRef]